Supplement of Atmos. Meas. Tech., 15, 6935–6947, 2022
https://doi.org/10.5194/amt-15-6935-2022-supplement

Supplement of

Online measurements of cycloalkanes based on NO^+ chemical ionization in proton transfer reaction time-of-flight mass spectrometry (PTR-ToF-MS)

Yubin Chen et al.

Correspondence to: Bin Yuan (byuan@jnu.edu.cn)

Normalization the measurement data of NO+ PTR-ToF-MS

Here we normalize the raw data measured by NO^+ PTR-ToF-MS in the following way:

$$i[RH^+]_{norm} = \frac{i[RH^+]}{i[NO^+]} \times 10^6 \qquad (S1)$$

In this equation, $i[RH^+]_{norm}$ represents the signal value of normalized measurement data (ncps), $i[RH^+]$ represents the signal value of original measurement data (cps), nd $i[NO^+]$ represents the ion abundance of NO^+ ions. The $i[NO^+]$ is calculated from the ratio between ^{14}N and its isotopes ^{15}N, which is defined at 277 in this study.

Calculation method of instrument detection limit

The detection limit is the minimum concentration of the compounds that can be detected by the instrument and is related to the response factor, integration time, background signal and signal-to-noise ratio of the compounds to be tested. Assuming that both the statistical characteristic of the signal and the random error (noise) conform to the Poisson distribution, then according to the error transfer formula, the signal-to-noise atio can be expressed as:

$$\frac{S}{N} = \frac{C_f\,[X]\,t}{\sqrt{C_f[X]\,t + 2\,B\,t}} \qquad (S2)$$

where B represents the background signal, C_f is the calibration response factor, [X] represents the detection limit, and t is the integration time.The detection limit of cycloalkanes measured by NO^+ PTR-ToF-MS are calculated as the concentrations at which signal counts are 3 times the SD of measured background counts (Bertram et al., 2011; Wang et al., 2020; Yuan et al., 2017).

Table S1. Detailed information of the customized cylinder gas standard used in this study.

Standard Compound	Formula	CAS#	Concentration (ppb)	Uncertainty
Toluene	C_7H_8	108-88-3	101.7	±5%
Methacrolein	C_4H_6O	78-85-3	103.7	±5%
1,1,3,5-Tetramethylcyclohexane	$C_{10}H_{20}$	4306-65-4	100.5	±5%
Pentylcyclohexane	$C_{11}H_{22}$	4292-92-6	95.9	±5%
Hexylcyclohexane	$C_{12}H_{24}$	4292-75-5	96.0	±5%
Heptylcyclohexane	$C_{13}H_{26}$	5617-41-4	100.0	±5%
Octylcyclohexane	$C_{14}H_{28}$	1795-15-9	74.6	±5%
Octane	C_8H_{18}	111-65-9	100.8	±5%
Nonane	C_9H_{20}	111-84-2	100.1	±5%
Decane	$C_{10}H_{22}$	124-18-5	100.7	±5%
Undecane	$C_{11}H_{24}$	1120-21-4	97.4	±5%
Dodecane	$C_{12}H_{26}$	112-40-3	98.2	±5%
Tridecane	$C_{13}H_{28}$	629-50-5	99.4	±5%
Tetradecane	$C_{14}H_{30}$	629-59-4	96.0	±5%
Penadecane	$C_{15}H_{32}$	629-62-9	27.9	±5%

Table S2. Detailed information of the measurement location and technique used for detection of cycloalkanes in this study and previous studies.

Measurement location	Measuring technique	Reference
Guangzhou, China	NO^+ PTR-ToF-MS	This work
Algiers, Algeria	High-resolution gas chromatography-mass spectrometry (GC-MS) [a]	(Yassaa et al., 2001)
Los Angeles, USA	A two-channel in situ gas chromatography-mass spectrometry (GC-MS/FID) [a]	(de Gouw et al., 2017)
London, UK	Two-dimensional gas-chromatography time-of flight mass- spectrometry (TD-GC×GC ToF-MS) [b]	(Xu et al., 2020)
Northeastern Colorado, USA	GC-MS/FID [a]	(Gilman et al., 2013)
Lubricating oils	TD-GC×GC ToF-MS [b]	(Liang et al., 2018)
Diesel exhausts	TD-GC×GC ToF-MS [b]	(Alam et al., 2016)
Gasoline and diesel exhausts	GC-MS [c]	(Gentner et al., 2012)
Gasoline and diesel exhausts	NO^+ PTR-ToF-MS	This work

[a] The reported acyclic and cyclic alkanes were identified and quantified with gas standards

[b] The total ions signals of species is integrated into different regions (bin) according to the residence time of *n*-alkanes. The total ions signals of each bin were considered as the signals of acyclic and cyclic alkanes.

[c] The total ions signals of acyclic and cyclic alkanes were calculated by subtracted the signals of known compounds from similar chemical classes, and the remaining signals were considered to be the signals of acyclic and cyclic alkanes.

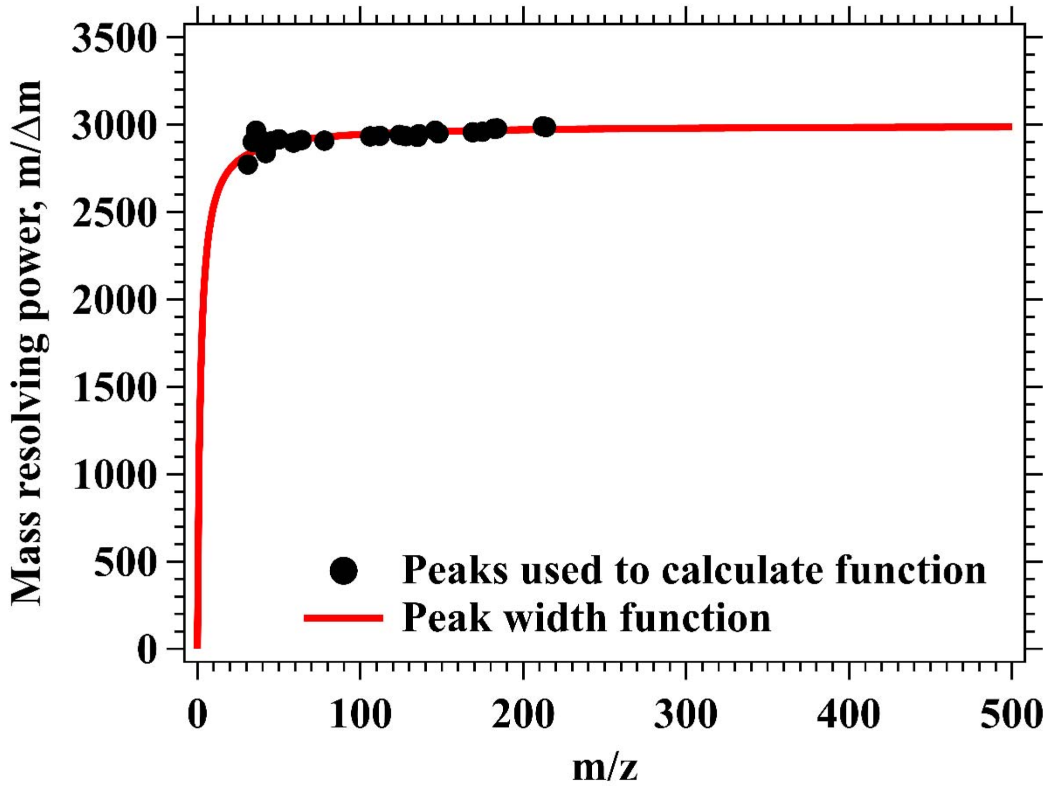

Figure S1. The relationship between mass resolving power and m/z.

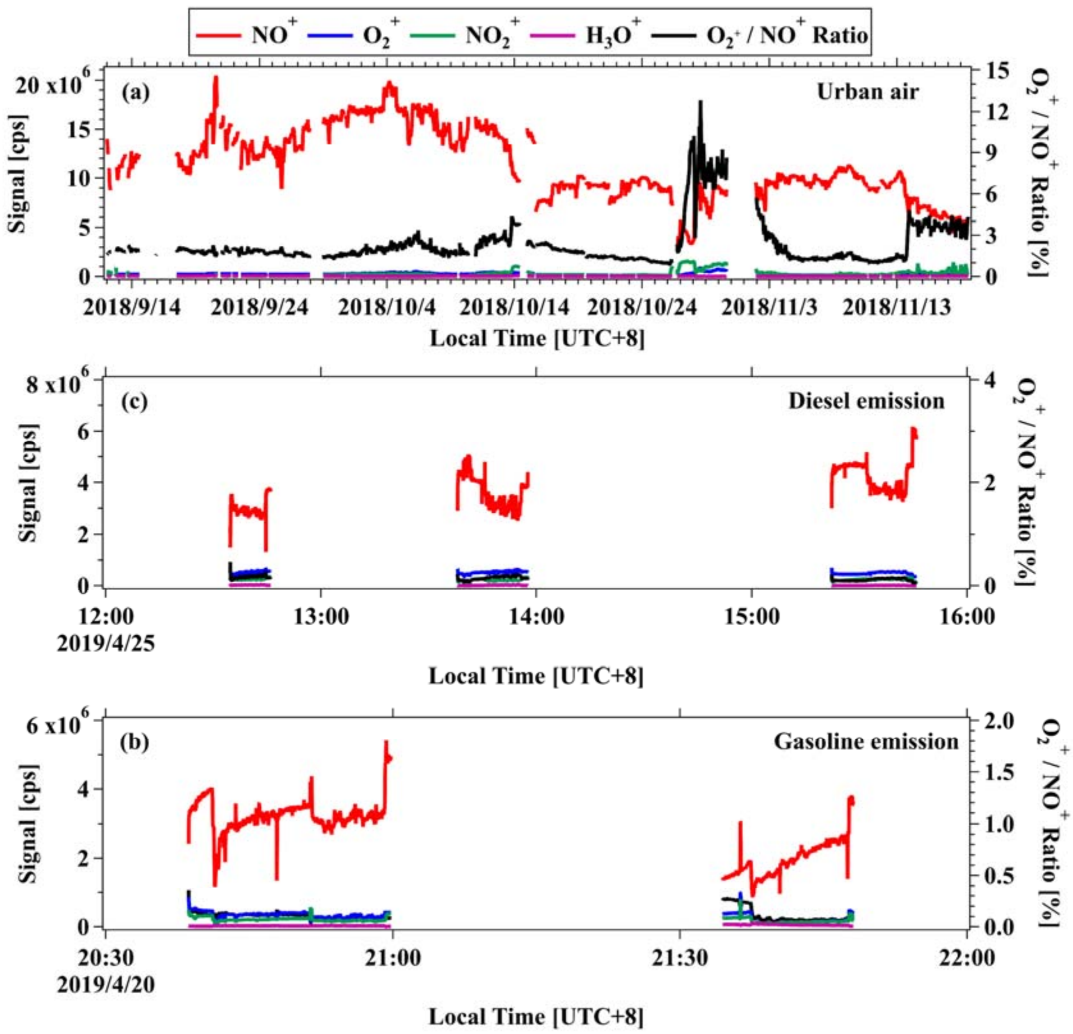

Figure S2. Time series of NO^+, O_2^+, NO_2^+, and $H_3O^+$and the ratio of O_2^+ to NO^+ during the measurement of urban air **(a)** and vehicular emissions **(b-c)**.

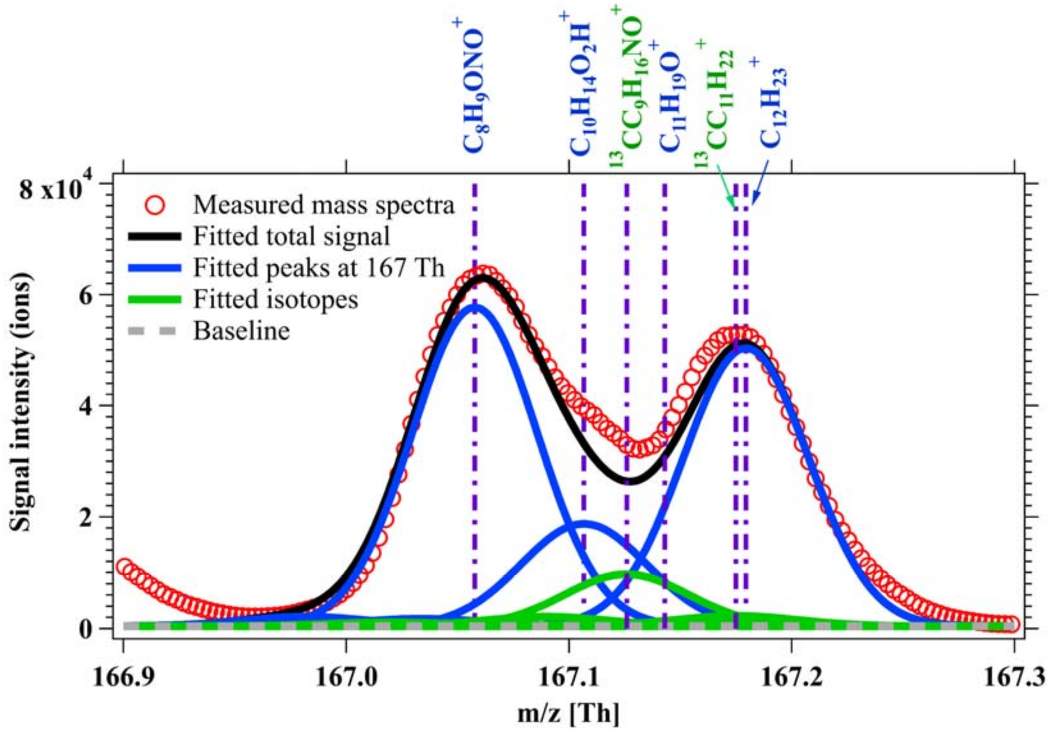

Figure S3. High-resolution peak fitting to the averaged mass spectra on a typical day (6 October 2018) for *m/z* 167 to individual ion peaks of C_{12} cycloalkanes ($C_{12}H_{23}^+$), other isomeric ions ($C_8H_9ONO^+$,$C_{10}H_{14}O_2H^+$, and $C_{11}H_{19}O^+$), and isotopes of other ion ($^{13}CC_9H_{16}NO^+$ and $^{13}CC_{11}H_{22}^+$) detected from NO^+ PTR-ToF-MS.

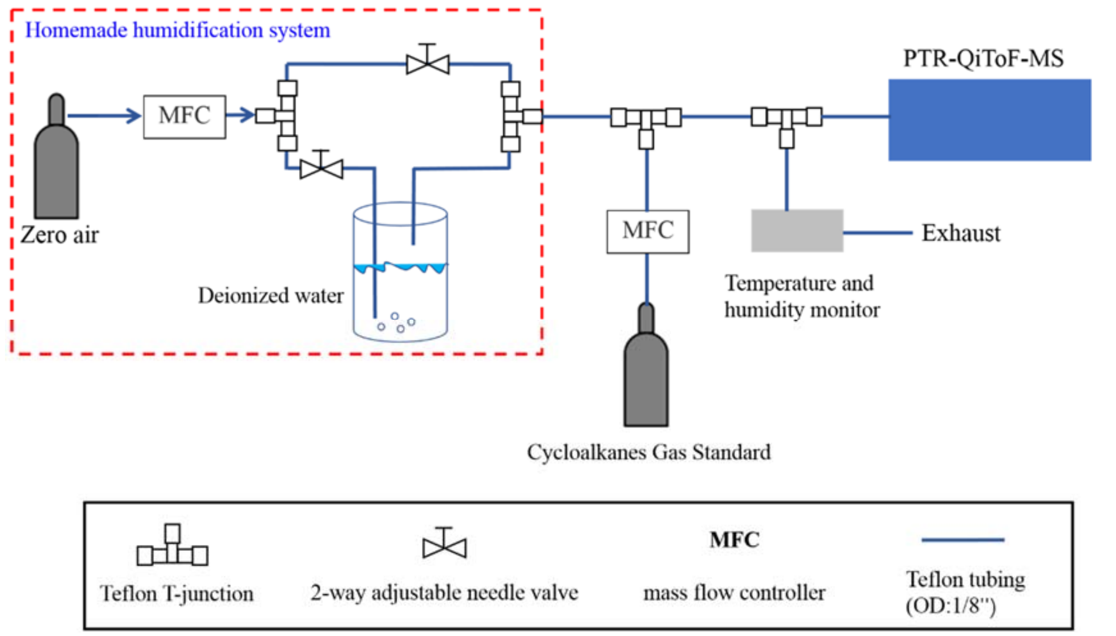

Figure S4. Schematic drawing of the custom-built humidity delivery system.

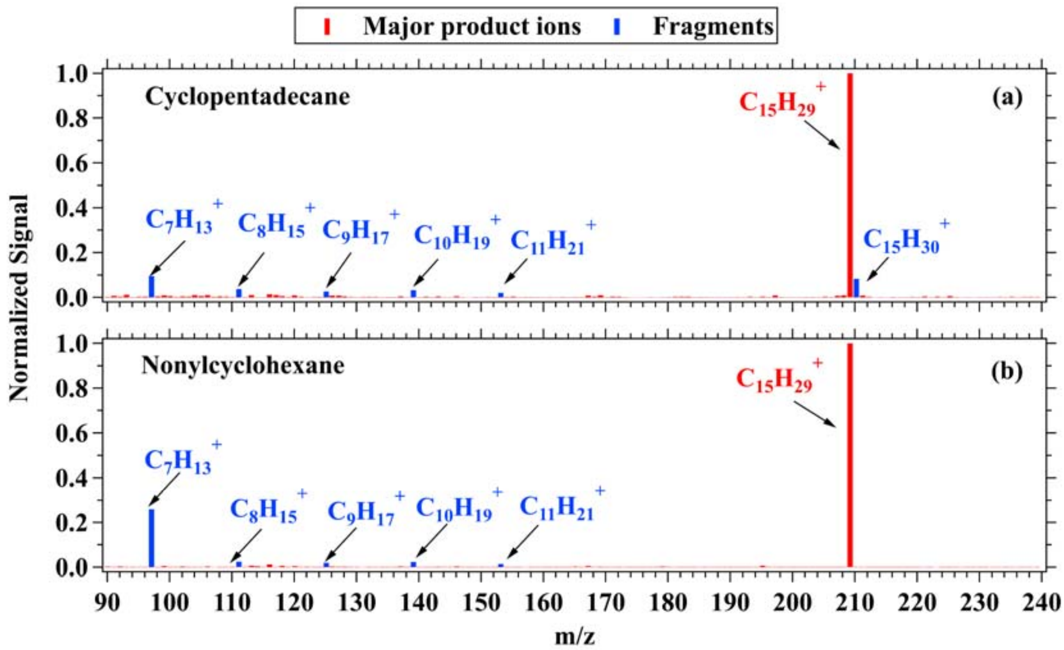

Figure S5. Mass spectra of product ions from cyclopentadecane **(a)** and nonylcyclohexane **(b)** in NO^+ PTR-ToF-MS. The major product ions are shown in red, and the fragments are sown in blue.

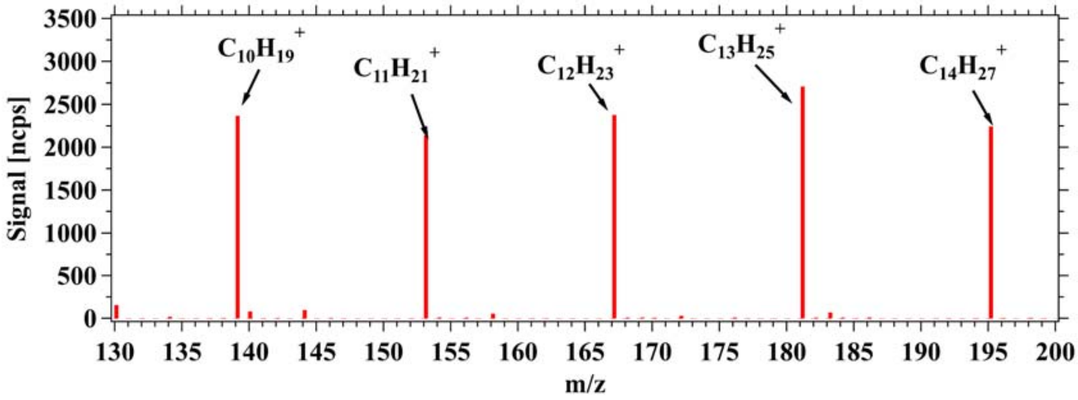

Figure S6. Mass spectra of product ions from C_{10}-C_{14} alkyl-cyclohexanes in NO^+ PTR-ToF-MS during the calibration experiments.

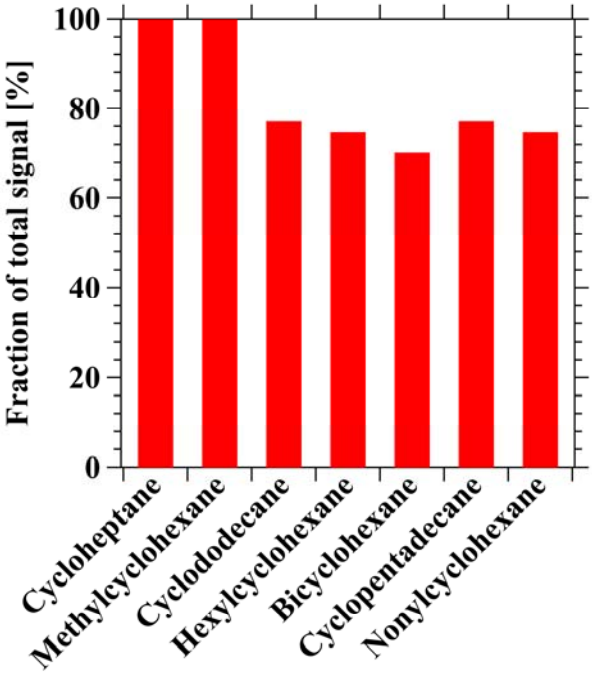

Figure S7. The fractions of product ions (M-H) from hydride abstraction of C_7, C_{12}, and C_{15} cyclic alkanes and C_{12} bicyclic alkanes in NO^+ PTR-ToF-MS.

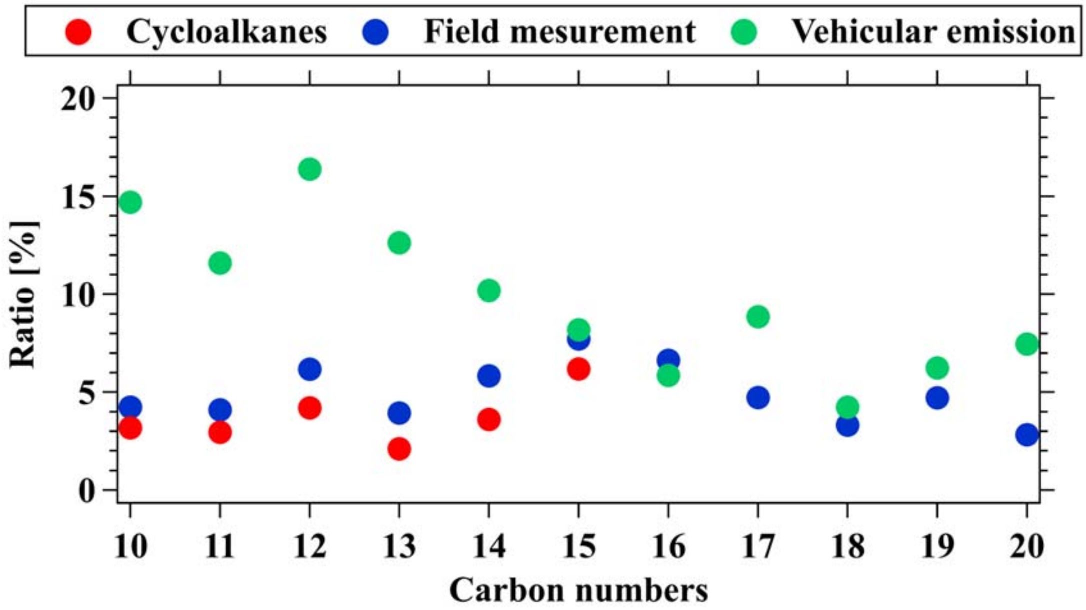

Figure S8. The ratios of $C_nH_{2n}^+$ to $C_nH_{2n-1}^+$ from cycloalkanes (red), field measurement (blue) and vehicular emissions (green) measured by NO^+ PTR-ToF-MS.

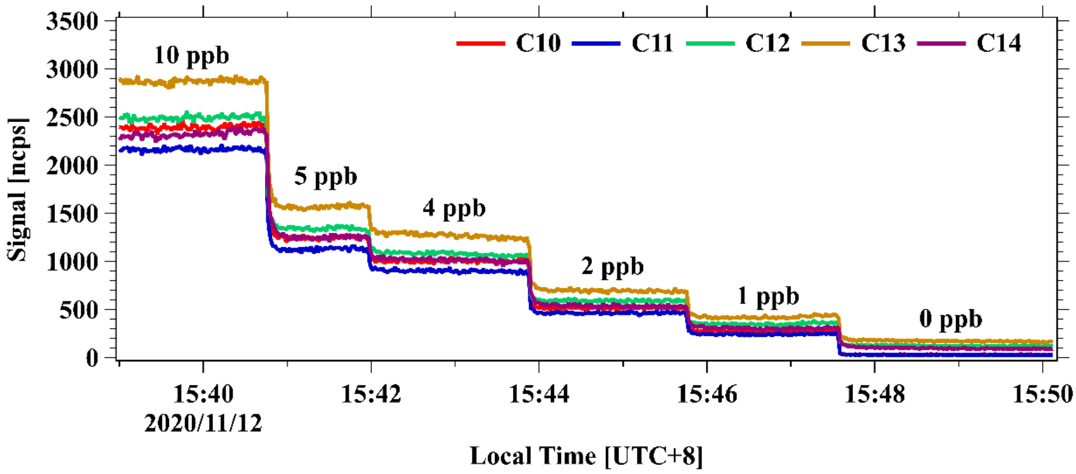

86

87 **Figure S9.** The multipoint calibrations of C_{10}-C_{14} cycloalkanes in dry condition (<1%

88 RH).

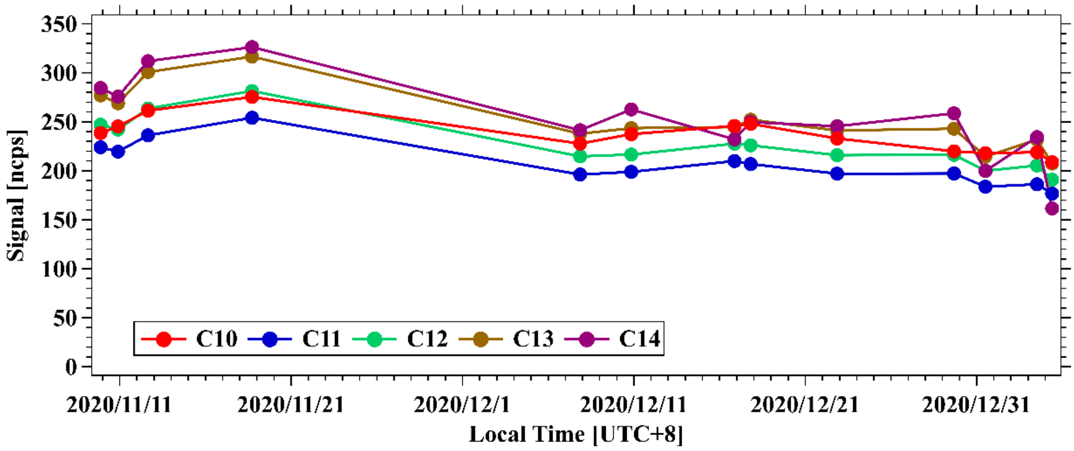

Figure S10. Calibration results of NO^+ PTR-ToF-MS for C_{10}-C_{14} cycloalkanes during the laboratory experiments.

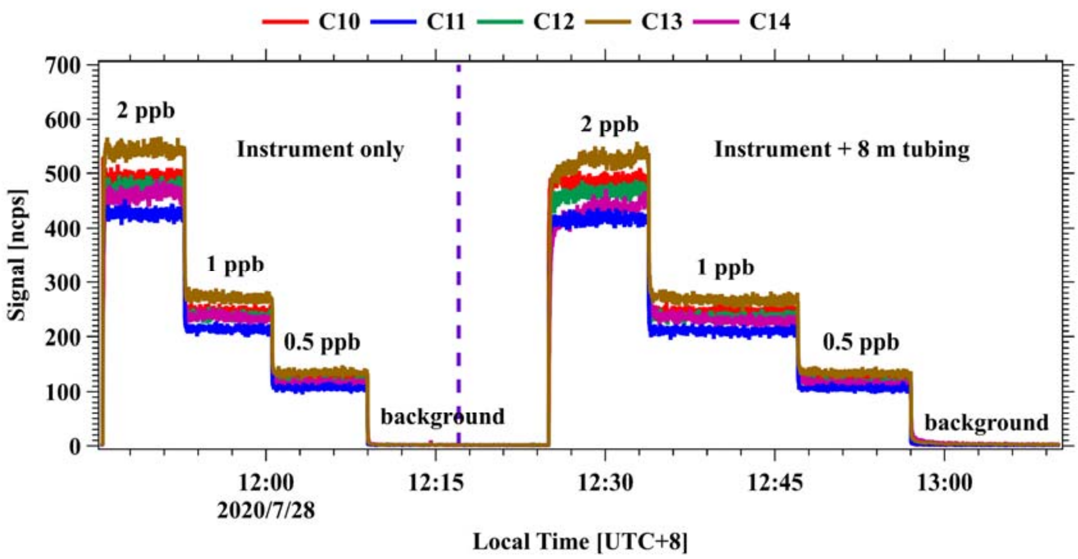

92

93 **Figure S11.** The tubing loss experiments of cycloalkanes (C_{10}-C_{14}) measured by NO^+

94 PTR-ToF-MS with an external pump at 5.0 L/min.

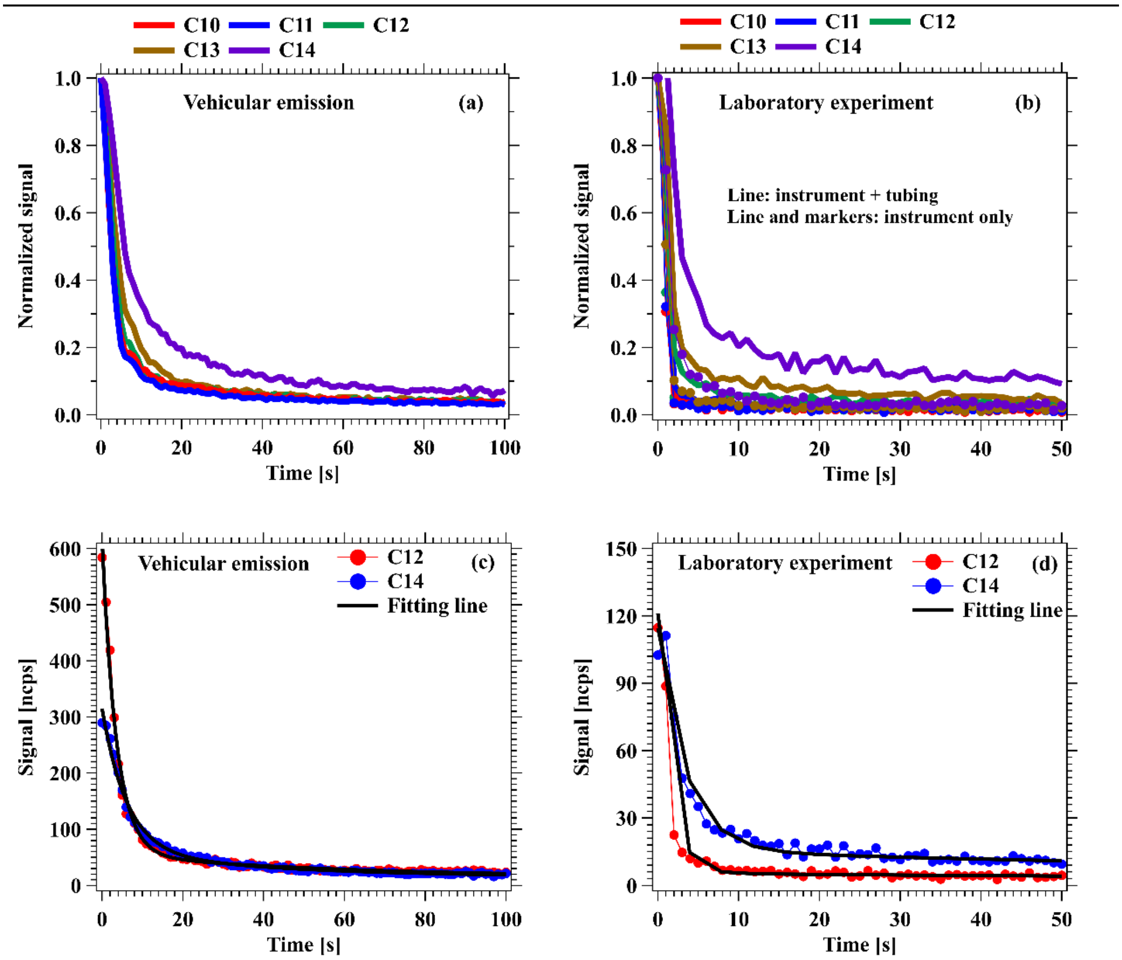

Figure S12. (a) The decrease in the normalized signal of cycloalkanes during the vehicular emission measurement. **(b)** The decrease in the normalized signal of cycloalkanes for instrument + tubing (line) and instrument only (line and markers) during the laboratory experiments. **(c-d)** The decrease in the signal of C_{12} and C_{14} cycloalkanes during the vehicular emission test and laboratory experiments, respectively. The data are fitted by a hyperbolic equation.

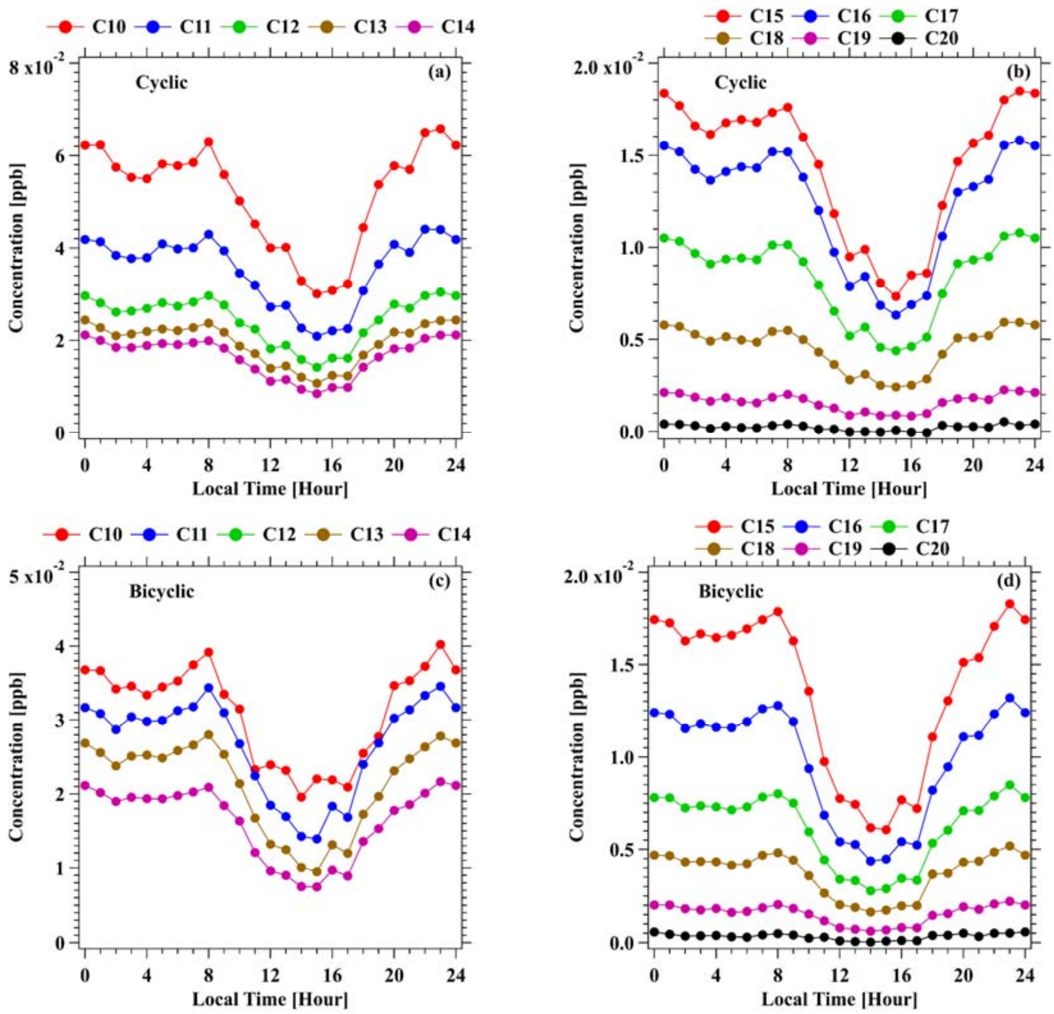

Figure S13. Diurnal variations of C_{10}-C_{20} cyclic and bicyclic alkanes during the campaign in urban region.

Reference

Alam, M. S., Zeraati-Rezaei, S., Stark, C. P., Liang, Z., Xu, H., and Harrison, R. M.: The characterisation of diesel exhaust particles – composition, size distribution and partitioning, Faraday Discussions, 189, 69-84, 2016.

Bertram, T. H., Kimmel, J. R., Crisp, T. A., Ryder, O. S., Yatavelli, R. L. N., Thornton, J. A., Cubison, M. J., Gonin, M., and Worsnop, D. R.: A field-deployable, chemical ionization time-of-flight mass spectrometer, Atmospheric Measurement Techniques, 4, 1471-1479, 2011.

de Gouw, J. A., Gilman, J. B., Kim, S. W., Lerner, B. M., Isaacman-VanWertz, G., McDonald, B. C., Warneke, C., Kuster, W. C., Lefer, B. L., Griffith, S. M., Dusanter, S., Stevens, P. S., and Stutz, J.: Chemistry of Volatile Organic Compounds in the Los Angeles basin: Nighttime Removal of Alkenes and Determination of Emission Ratios, Journal of Geophysical Research: Atmospheres, 122, 11,843-811,861, 2017.

Gentner, D. R., Isaacman, G., Worton, D. R., Chan, A. W., Dallmann, T. R., Davis, L., Liu, S., Day, D. A., Russell, L. M., Wilson, K. R., Weber, R., Guha, A., Harley, R. A., and Goldstein, A. H.: Elucidating secondary organic aerosol from diesel and gasoline vehicles through detailed characterization of organic carbon emissions, Proceedings of the National Academy of Sciences of the United States of America, 109, 18318-18323, 2012.

Gilman, J. B., Lerner, B. M., Kuster, W. C., and de Gouw, J. A.: Source Signature of Volatile Organic Compounds from Oil and Natural Gas Operations in Northeastern Colorado, Environmental Science & Technology, 47, 1297-1305, 2013.

Liang, Z., Chen, L., Alam, M. S., Zeraati Rezaei, S., Stark, C., Xu, H., and Harrison, R. M.: Comprehensive chemical characterization of lubricating oils used in modern vehicular engines utilizing GC × GC-TOFMS, Fuel, 220, 792-799, 2018.

Wang, C. M., Yuan, B., Wu, C. H., Wang, S. H., Qi, J. P., Wang, B. L., Wang, Z. L., Hu, W. W., Chen, W., Ye, C. S., Wang, W. J., Sun, Y. L., Wang, C., Huang, S., Song, W., Wang, X. M., Yang, S. X., Zhang, S. Y., Xu, W. Y., Ma, N., Zhang, Z. Y., Jiang, B., Su, H., Cheng, Y. F., Wang, X. M., and Shao, M.: Measurements of higher alkanes using NO^+ chemical ionization in PTR-ToF-MS: important contributions of higher alkanes to secondary organic aerosols in China, Atmospheric Chemistry and Physics, 20, 14123-14138, 2020.

Xu, R., Alam, M. S., Stark, C., and Harrison, R. M.: Composition and emission factors of traffic- emitted intermediate volatility and semi-volatile hydrocarbons (C_{10}–C_{36}) at a street canyon and urban background sites in central London, UK, Atmospheric Environment, 231, 2020.

Yassaa, N., Meklati, B. Y., Brancaleoni, E., Frattoni, M., and Ciccioli, P.: Polar and non-polar volatile organic compounds (VOCs) in urban Algiers and saharian sites of Algeria, Atmospheric Environment, 35, 787-801, 2001.

Yuan, B., Koss, A. R., Warneke, C., Coggon, M., Sekimoto, K., and de Gouw, J. A.:

Proton-Transfer-Reaction Mass Spectrometry: Applications in Atmospheric Sciences, Chem Rev, 117, 13187-13229, 2017.